Department of Veterans Affairs

Journal of Rehabilitation Research and Development Vol. 38 No. 1, January/February 2001
Pages 129–133

SLO power calibration

Rolf W. Nygaard, PhD and Ronald A. Schuchard, PhD
Department of Ophthalmology, University of Missouri-KC, Kansas City, MO; VA Rehab R&D Center and Emory University School of Medicine, Decatur, GA 30322

Abstract—We present a method for calibrating the Scanning Laser Ophthalmoscope (SLO) that predicts radiant power at any of 256 grayscale values (gsv) and 12 polarized filter (polarizer) levels. Predicted power values, p(gsv), were determined by substitution into polynomials linearly transformed to old or new power at p(0) and p(255). This was compared with observed power values at 125 levels of attenuation/session. Prediction accuracy was the proportion of nonsignificant pairwise comparisons (t-test, p=0.0001). We found that power transformation between polarizers and within sessions has both linear and nonlinear characteristics. Within polarizer and between sessions, however, power transformation has linear characteristics. A 5th-degree polynomial was individually fit, at each polarizer, to session 1 power distributions of 9 gsv steps (0, 31, 63, 95, 127, 159, 191, 223, 255). When adjusted to p(255) and p(0) in new sessions, we obtained p(gsv) that predicted power at 25 gsv * 5 polarizers for 18 days with an accuracy of about 0.84. When only adjusted to p(255), predictive accuracy was 0.81.

Key words: *calibration, computer, laser, ophthalmoscopy, SLO.*

This material is based upon work supported in part by VA Rehabilitation, Research, & Development Service grant #C838-RA1 and The Eye Foundation of Kansas City..

Address all correspondence and requests for reprints to: Rolf W. Nygaard, PhD, Department of Vision Sciences, Children's Mercy Hospital, 2401 Gilham Road, Kansas City, MO 64108; email: rnygaard@cmh.edu.

INTRODUCTION

The Scanning Laser Ophthalmoscope (SLO) has been used for perimetry, fixation, pursuit, acuity, and contrast sensitivity evaluations where precise control of visible stimulus presentations on the retina is essential (1–12). A typical instrument (we tested SLO model #101, Rodenstock, Germany) scans visible flux from a HeNe laser (633 nm) directly onto the retina. The laser beam is power attenuated, converged at the beam pivot (positioned in the patient's natural pupil), then diverged onto the patient's retina (13). Therefore, all available power from the SLO is manifest at the beam pivot.

Power attenuation occurs in two successive stages. First, a filter-polarizer pair (polarizer) sets the power level range (minimum to maximum) of the entire SLO field at one of 12 levels (from 0–11). Next, an acousto-optic modulator further attenuates the power of each individual pixel element through 256 grayscale values (gsv=0–255). A device internal to the SLO unit is designed to measure radiant power, but only at gsv 255. Determining values of radiant power in a clinical-evaluation study requires external measurement of power *versus* gsv with polarizer level as parameter. The power should be repeatedly measured to average out noise. Much time and effort would be saved if empirical plots of power variation with gsv regressed onto a single polynomial

function that predicted power variation with beam attenuation. For linear variation with polarizer, a single curve fit for all polarizers would suffice. Nonlinear variation, however, would require separate fits at all 12 polarizers. We will investigate (1) whether the polarizer transformation of power as a function of gsv is indeed linear, (2) how predictive accuracy varies with polynomial degree, (3) how predictive accuracy varies with time, and (4) the smallest number of gsv steps required to be measured and fitted for maximum predictive accuracy.

METHODS

Radiant power measurements were made at the SLO beam pivot with an LM-2 CW detector (Coherent Optics, Inc.) attached to a Labmaster digital processor—PC couple. The processor provided analog-digital conversion; the PC provided control of scan and gsv as well as data acquisition, storage, and analysis. We examined a second Generation SLO using full-field, uniform raster scan. (Results were corroborated in a Generation 3 SLO and in an upgraded Generation 1 SLO.) The power-sampling period was 100 ms, exceeding the time required to complete full-field scan (30 ms). **Figure 1** schematizes the arrangement.

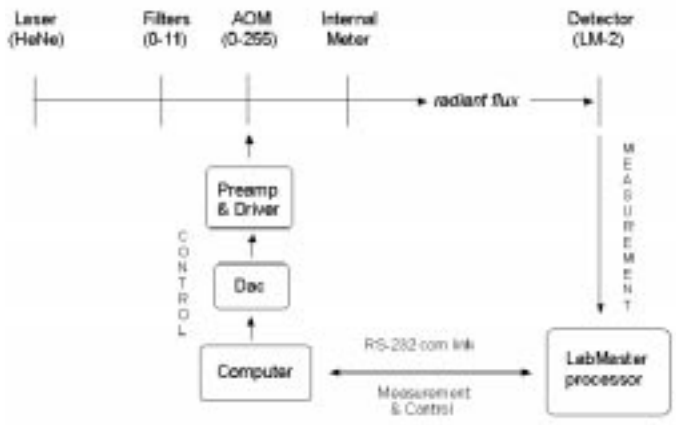

Figure 1.
Instrumentation for control and measurement of the SLO.

Between increments in gsv, a 2-second interval was introduced to provide for stabilization of power output. Within a given measurement session, power was measured at 25 gsv steps (distributed in equal-interval between steps 0 and 255) (14). This was performed in ascending numerical order, repeated for a total of 20 measurements (intended to average out noise), and repeated again at each of 5 different polarizers (3, 5, 7, 9, and 11: a sample of the entire SLO polarizer range). Including the delay required for polarizer change (about 5 seconds), the total time required to complete a measurement session was: ((2 seconds/gsv * 25 gsv * 20 repetitions/polarizer) + 5 seconds) * 5 polarizers=83.75 minutes. In all, five measurement sessions were performed (on days 1, 2, 8, 11, and 18).

Data collection and analysis were performed in 8 stages.

1. Acquisition of repeated SLO power measures.
2. Calculation of averages and standard deviations across each gsv for each polarizer and measurement session. Power averages from all five measurement sessions defined the power-gsv distribution and, with no further alteration, provided our "observed power." At the same time, from the power averages of session 1 we obtained predicted power, "p(gsv)." This procedure was performed in stages 3–6.
3. Length reduction of session 1 power averages. Points at gsv 0 and 255 were retained while those corresponding to every other gsv step, step pair, or step triplet were eliminated. This yielded four different lengths of 25, 13, 9, and 7 equal-interval steps.
4. Adjustment of their distributions to align minimum and maximum points. Distributions were first translated so 0 gsv corresponded with 0 power (zero-translation), and then normalized so that 255 gsv corresponded with unity. This adjustment defines a linear transformation (translation and division by a constant) of the power distribution that might occur from a change in either polarizer or session. By reversing the order (multiplying by a new polarizer-session maximum and then translating to a new polarizer-session minimum) we linearly reconstitute the power distribution.
5. Polynomial regression of the zero-translated and normalized distribution to obtain best-fitting regression coefficients.
6. Linear reconstitution of the polynomial using one of four rescaling protocols: multiplication of the polynomial by the maximum power from either the first session ("old p(255)") or from some later session ("new p(255)") followed by translation of the polynomial to

the power minimum of either the first ("old p(0)") or some later session ("new p(0)"). This provided us with values of p(gsv).

7. Statistical comparison of power distributions between polarizers, performed by t-test pairwise comparisons (15) of adjusted session 1 power distributions over 10 polarizer pair combinations. The two distributions were assumed normal, with identical population variances estimated from the variances of repeated measures. We defined a significant (p=0.0001) difference to indicate an incorrect match or prediction and a nonsignificant difference to indicate a correct match or prediction. Match accuracy was the proportion of nonsignificant differences out of 25 comparisons (25 gsv/polarizer).
8. Statistical comparison between p(gsv) and observed power performed by t-test pairwise comparisons (15) of between-session predicted and observed power distributions over five measurement sessions. Observed power was assumed normal and its variance was estimated from the variance of repeated measures. Again, we defined a significant (p=0.0001) difference to indicate an incorrect match or prediction and a non-significant difference to indicate a correct match or prediction. Predictive accuracy was the proportion of nonsignificant differences out of 125 comparisons (25 gsv/polarizer * 5 polarizers).

RESULTS

First, we examined change in power within session and between polarizers. We compared distributions that were linearly transformed by either normalizing and translating or just normalizing. Significant differences at gsv other than 0 and 255 would indicate a nonlinear transformation and would require separate curve fits at each polarizer.

Translated and normalized data for measurement session 1 (typical of all later sessions) are shown in **Figure 2a**. Significant differences exist between polarizers. **Figure 2b** details this by showing the proportion of nonsignificant power matches (match accuracy) at each of 10 polarizer combinations. Results for both translated and normalized or only normalized data are shown. High match accuracy (0.80 to 1.00) is shown for polarizer combinations 5–7, 5–9, 7–9, 7–11, and 9–11; much lower accuracy (0.04 to 0.44) is shown for the other 5 pairs (3–5, 3–7, 3–9, 3–11, 5–11). Thus, for half our polarizer combinations, a linear transformation is insufficient to account for power change with polarizer. Because there was perfect match accuracy (1.00) at only one polarizer combination (5–7), we decided to curve-fit at each polarizer level.

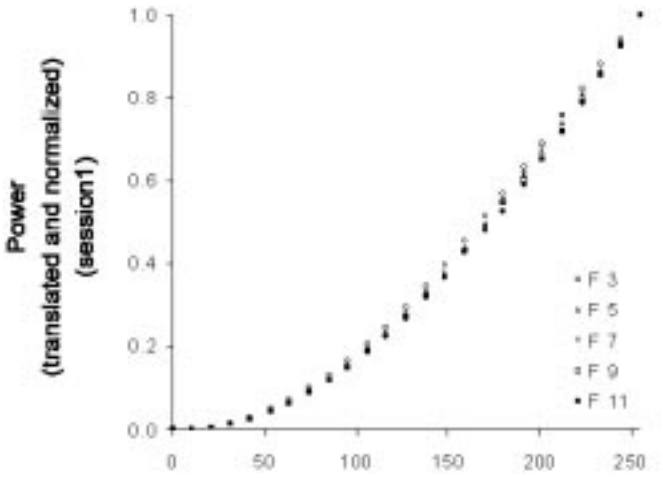

Figure 2a.
Power at 25 gsv (from 0–255) and 5 polarizers (F=3, 5, 7, 9, 11) in measurement session 1 translated (to 0 power at 0 gsv) and normalized (to power at 255 gsv). At numerous gsv, power changes significantly between polarizers.

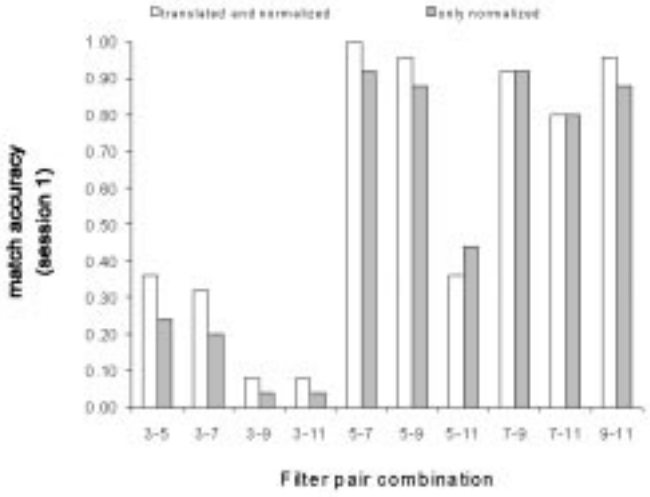

Figure 2b.
Calculation of match accuracies for each of 10 polarizer pair combinations. A linear transformation can account for most or all match discrepancy in about half the polarizer combinations. For the remaining half, however, a linear transformation is insufficient.

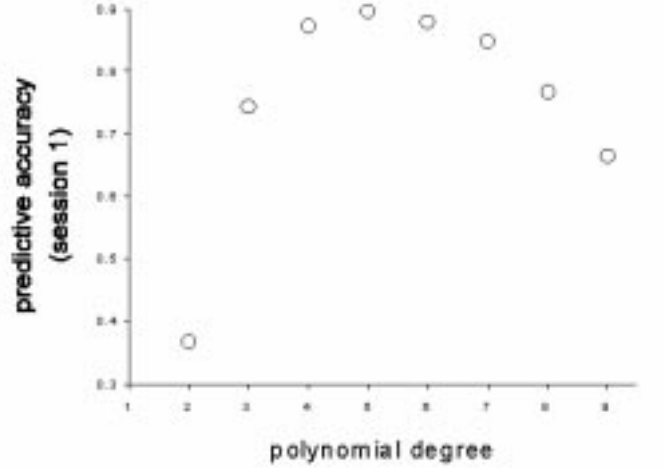

Figure 3.
The accuracy of polynomials fit to observed session 1 power to predict those values. Polynomial degree ranged from 2 through 9. Greatest accuracy (0.90) was obtained at degree 5.

Next, we determined the polynomial degree that maximized predictive accuracy. **Figure 3** shows how predictive accuracy varies with polynomial degree (2–9). We see that accuracy is a maximum (0.90) for polynomials of degree 5 and declines at both higher and lower values. Therefore, 0.90 is the maximum predictive accuracy attainable by polynomial simulation of our power data.

Finally, we examined change in power between sessions, within polarizer and determined the minimum number of gsv needed in regression. **Figure 4** shows the predictive accuracy provided by each of our four rescaling protocols in each of five measurement sessions. In session 1, all protocols converge to a predictive accuracy of 0.90 (predicted and observed sessions are the same). In subsequent sessions, however, two trends are apparent. For protocols using old p(255) predictive accuracy declines below 0.20 and for protocols using new p(255) predictive accuracy remains above 0.74. This is true regardless of whether the protocol uses new p(0) or old p(0). Within filter and between session power changes linearly with gsv. We conclude there are linear power changes over sessions that are specified by a change in the maximum power.

Figure 5 shows predictive accuracy (averaged over sessions 1–5) of polynomials fit to gsv lengths of 7, 9, 13, and 25 steps. The greatest accuracy (0.84) occurs with fits to a power distribution length of 9 gsv using a rescaling protocol of new p(0) and new p(255). When old p(0) and new p(255) are used instead, however, predictive accuracy is only slightly lower (0.81), reinforcing the earlier finding that linear power changes occur over sessions and are specifiable by a change in the maximum power.

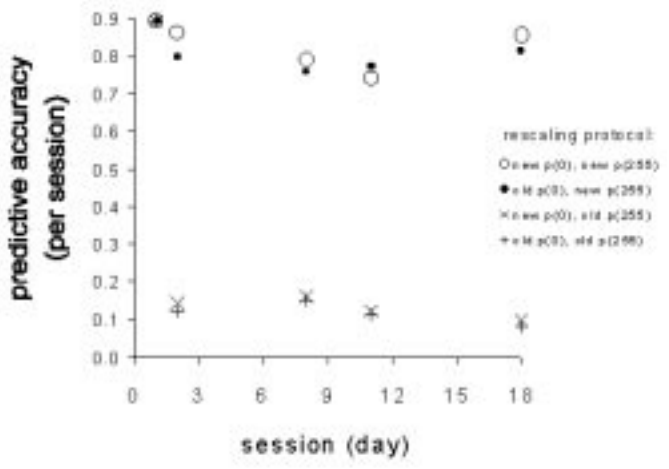

Figure 4.
Duration of predictive accuracy for polynomials of degree 5. Polynomials were linearly adjusted by one of four rescaling protocols (see figure legend). Over 18 days, prediction accuracy is approximately the same regardless of whether polynomials are adjusted to new session maxima and new session minima, or just adjusted to new session maxima. See text for details.

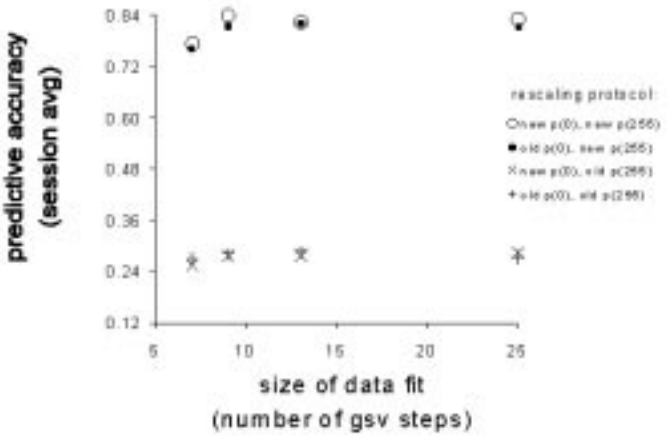

Figure 5.
Predictive accuracy averaged over all sessions (days 1, 2, 8, 11, and 18). Polynomials of degree 5 were fit to power distributions of 7, 9, 13, or 25 equal-interval gsv and 5 polarizer values. Polynomials were linearly adjusted in one of four rescaling protocols (see figure legend). Maximum predictive accuracy was achieved with only 9 gsv. See text for details.

CONCLUSION

We propose that a 5th-degree polynomial fit to a normalized power distribution of 9 gsv steps (0, 31, 63, 95, 127, 159, 191, 223, 255) for each individual polarizer and then multiplied into new maxima (p(255)) on future sessions, will predict power at any of 256 gsv steps

and 12 polarizers for at least 18 days with an accuracy of about 0.81.

Accurately and efficiently relating SLO radiant power to the settings of laser beam attenuation is essential for visual function evaluation. The ability to accurately set SLO power is especially critical for research and clinical testing of scotoma density and contrast sensitivity. The reliability of SLO power over time is also essential for long-term studies that monitor progression of scotomas and other visual impairment due to ocular disease such as age-related macular degeneration. However, none of the previous long-term SLO studies cited reported how the variability of SLO power was controlled (16–18). Indeed, many of the previous SLO studies have not even acknowledged in their visual function testing the variability in power that we report. Thus, comparing studies or attempting to replicate previously reported studies might be difficult if not impossible. Differences in reported visual function values should be due to changes in retinal and not instrumental function.

ACKNOWLEDGMENTS

The authors wish to thank Mr. Wen-Te-Lin for valuable technical assistance with computer hardware and software.

REFERENCES

1. Culham LE, Fitzke FW, Timberlake GT, Marshall J. Use of scrolled text in a scanning laser ophthalmoscope to assess reading performance at different retinal locations. Ophthalmic Physiol Opt 1992;12:281–6.
2. Culham LE, Fitzke FW, Timberlake GT, Marshall J. Assessment of fixation stability in normal subjects and patients using a scanning laser ophthalmoscope. Clin Vis Sci 1993;8:551–61.
3. Fletcher DC, Schuchard RA. Preferred retinal loci relationship to macular scotomas in a low vision population. Ophthalmology 1997;104:632–8.
4. Guez JE, Le Gargasson JF, Rigaudiere F, O'Regan JK. Is there a systematic location for the pseudo-fovea in patients with central scotoma? Vision Res 1993;33:1271–9.
5. Lei H, Schuchard RA. Using two PRLs for different lighting conditions in patients with central scotomas. Invest Ophthalmol Vis Sci 1997;38:1812–8.
6. Remky A, Beausencourt E, Elsner AE. Angioscotometry with the scanning laser ophthalmoscope: comparison of the effect of different wavelengths. Invest Ophthalmol Vis Sci 1996;37:2350–5.
7. Rubin GS, Turano K. Low vision reading with sequential word presentation. Vision Res 1994;34:1723–33.
8. Schuchard RA, Fletcher DC. Preferred retinal locus: a review with applications in low vision rehabilitation. Ophthalmol Clin N Am 1994;7:243–55.
9. Schuchard RA, Raasch TW. Retinal locus for fixation: pericentral fixation targets. Clin Vis Sci 1992;7:511–20.
10. Sunness JS, Schuchard RA, Shen N, Rubin GS, Dagnelie G, Haselwood DM. Landmark-driven fundus perimetry using the scanning laser ophthalmoscope (SLO). Invest Ophthalmol Vis Sci 1995;36:1863–74.
11. Timberlake GT, Peli E, Essock EA, Augliere RA. Reading with a macular scotoma II. Retinal locus for scanning text. Invest Ophthalmol Vis Sci 1987;28:1268–74.
12. Trauzettel-Klosinski S, Tornow RP. Fixation behavior and reading ability in macular scotoma. Neuro-ophthalmol 1996;16:241–53.
13. Webb RH, Hughes GW. Scanning laser ophthalmoscope. IEEE Trans on Biomed Engineer. 1981;BME-28:438–92. Webb RH. Manipulating laser light for ophthalmology. IEEE Engineering in Medicine and Biology Magazine. December 1986:12–16. Webb RH, Hughes GW, Francois CD. Confocal scanning laser ophthalmoscope. Appl Optics 1987;26:1492–9.
14. The 25 gsv steps were: 0, 10, 21, 31, 42, 53, 63, 74, 85, 95, 106, 116, 127, 138, 148, 159, 170, 180, 191, 201, 212, 223, 233, 244, 255. The average interval between gsv steps (from 0 to 255) +/−1 SD was 10.6 +/−0.495 which is, approximately, equal-interval.
15. Sachs L. Applied statistics. New York: Springer-Verlag; 1984. pp. 136–7, Table 27 for determining limits of 2 tail significance, p. 135, Eq (1.128) for determining predictive accuracy, and p 265, Eq (3.27) for determining match accuracy.
16. Sunness JS, Bressler NM, Maquire MG. Scanning laser ophthalmoscopic analysis of the pattern of visual loss in age-related geographic atrophy of the macula. Am J Ophthalmol 1995;119:143–51.
17. Fletcher DC, Schuchard RA, Livingstone CL, Crane WG, Hu Sy. Scanning laser ophthalmoscope macular perimetry and applications for low vision rehabilitation clinicians. Ophthalmol Clin N Am 1994;7:257–65.
18. Guez JE, Le Gargasson JF, Massin P, Rigaudiere F, Grall Y, Gaudric A. Functional assessment of macular hole surgery by scanning laser ophthalmoscopy. Ophthamology 1996;105:694–9.

Submitted for publication May 2, 2000. Accepted in revised form August 15, 2000.